LETTER

Magnetoquantum oscillations in the specific heat of a topological Kondo insulator

Letters

IOP Publishing

Journal of Physics: Condensed Matter

J. Phys.: Condens. Matter **34** (2022) 36LT01 (6pp)

https://doi.org/10.1088/1361-648X/ac7d2b

Letter

Magnetoquantum oscillations in the specific heat of a topological Kondo insulator

P G LaBarre[1], A Rydh[2], J Palmer-Fortune[3], J A Frothingham[3], S T Hannahs[4], A P Ramirez[1] and N A Fortune[3,*]

[1] Department of Physics, University of California at Santa Cruz, Santa Cruz, CA 95064, United States of America
[2] Department of Physics, Stockholm University, Stockholm, SE-106 91, Sweden
[3] Department of Physics, Smith College, Northampton, MA 01063, United States of America
[4] National High Magnetic Field Laboratory, Florida State University, Tallahassee, FL 32310-3706, United States of America

E-mail: nfortune@smith.edu

Received 12 April 2022, revised 18 May 2022
Accepted for publication 29 June 2022
Published 6 July 2022

Abstract

Surprisingly, magnetoquantum oscillations (MQOs) characteristic of a metal with a Fermi surface have been observed in measurements of the topological Kondo insulator SmB_6. As these MQO have only been observed in measurements of magnetic torque (dHvA) and not in measurements of magnetoresistance (SdH), a debate has arisen as to whether the MQO are an extrinsic effect arising from rare-earth impurities, defects, and/or aluminum inclusions or an intrinsic effect revealing the existence of charge-neutral excitations. We report here the first observation of MQO in the low-temperature specific heat of SmB_6. The observed frequencies and their angular dependence for these flux-grown samples are consistent with previous results based on magnetic torque for SmB_6 but the inferred effective masses are significantly larger than previously reported. Such oscillations can only be observed if the MQO are of bulk thermodynamic origin; the measured magnetic-field dependent oscillation amplitude and effective mass allow us to rule out suggestions of an extrinsic, aluminum inclusion-based origin for the MQO.

Supplementary material for this article is available online

Keywords: heat capacity, composite fermions, de Haas–van Alphen effect, density of states, topological materials, spin fluctuations, quantum oscillations

(Some figures may appear in colour only in the online journal)

Despite five decades of study, the topological Kondo insulator SmB_6 continues to yield new physics, the most recent discovery being the observation of magneto-quantum oscillations (MQOs) characteristic of metals. The MQO are periodic in inverse magnetic field (1/H) and are field-angle dependent. Curiously, these oscillations are observed in measurements of the magnetic torque [1, 2] but not in charge transport

* Author to whom any correspondence should be addressed.

[3]. As a result, the physical origin of these oscillations continues to be debated. Arguments have been put forward in favor of an extrinsic origin dependent on impurities, defects, and/or sample growth methods [4, 5], a 2D surface state resulting from topological constraints [1, 6], and a 3D non-conducting metallic state [2, 7, 8] formed from a charge-neutral Fermi-liquid [9] charge-neutral excitons in a Kondo insulator [10, 11], or Majoranas in a mixed valence insulator [12].

With so many points still in contention, complementary thermodynamic probes of the quantum oscillations merit consideration. In particular, if the MQO do reflect an intrinsic and also bulk 3D thermodynamic property of the material (independent of growth conditions) then these oscillations must also occur in the specific heat of both flux-grown and float zone grown samples [12–14]. Indeed, MQO have been previously observed in specific heat measurements of very low carrier density semimetals [13, 14] and molecular conductors [15, 16].

For a normal metal, Lifshitz–Kosevich (L–K) theory predicts the magnitude of the quantum oscillations in the heat capacity for ordinary metals to be on the order of 0.1% of the ordinary electronic specific heat [13]. Our working assumption is that if the observed oscillatory behavior in SmB_6 arises from regions of the sample supporting large mean free paths of Fermi liquid-like excitations [12] then they will still be governed by L–K theory regarding oscillation amplitudes and frequencies, even if the material itself is an insulator and the excitations are charge neutral. We note, however, that some torque measurements [2, 7] exhibit MQO oscillations with an amplitude dependence differing from expectations of L–K theory below 1 K. Whether this is due to a field-dependent anisotropy—torque measures the anisotropy in M rather than M directly—or a violation of L–K theory is not clear at present. Thus our working assumption is a conservative approach to analyzing the data. In either case, the frequencies of oscillation are still in principle resolvable using Fourier analysis.

To investigate this possibility, we have measured the low temperature specific heat of both LaB_6 and SmB_6 as a function of applied magnetic field. For SmB_6, three separate flux-grown crystals of 0.43, 1.511, and 0.126 μg were compared, each grown in a separate batch at Los Alamos National Laboratory [17]. Our measurements of $C(T,H)$ were carried out using custom-built rotatable micro- and nano-calorimeters [18, 19] at $T<1$ K for magnetic fields up to 32 T and also as a function of temperature between 0.1 K and 100 K in magnetic fields up to 12 T. The heat capacities of the bare calorimeters were measured in separate runs and subtracted from the data; corrections were also made for the magnetoresistance of the thermometers [20].

In figure 1 we compare zero field and 12 T data for H $\|$ a axis, along with a representative fit to the 12 T data for a 0.430 μg sample. We note in the literature a large variation in the reported low temperature zero-field electronic specific heat γ values for different samples, so our primary interest here is in the magnetic field dependence of $\gamma(H)$ rather than the absolute value. Such a large sample-to-sample variation is unusual for most materials, but is characteristic of SmB_6 and may be

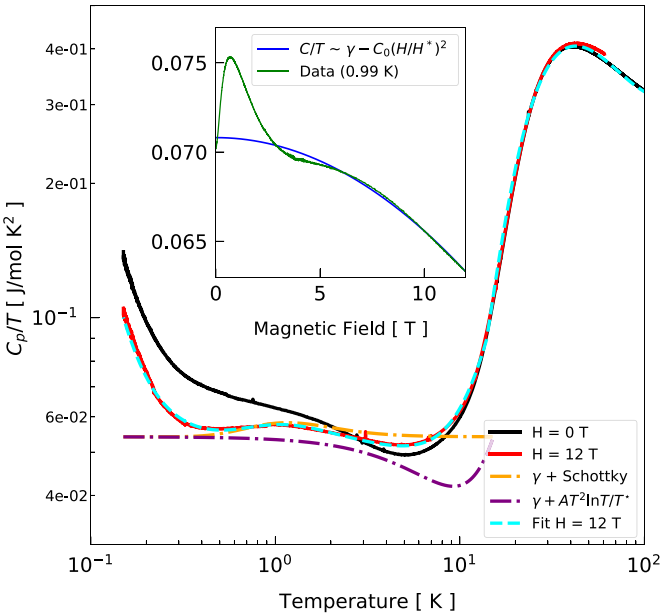

Figure 1. Temperature dependence of the specific heat at 0 T and 12 T for a 0.430 μg flux-grown SmB_6 sample, along with a representative fit to the temperature dependence at 12 T. Inset: field dependence of C/T at $T=0.99$ K. There is a Schottky peak near 1 T arising from magnetic impurities. The $T\ln T/T^*$ term and the low field $\gamma(0)(1-\alpha(H/H^*)^2$ field dependence are consistent with the presence of spin fluctuations with $T^*=15$ K ($H^*=23$ (T). $\gamma(H)$ is a constant above 28 T (not shown).

due to the variation in number and type of rare-earth impurities or in the density of mid-gap states [21].

Our results at both 0 T and 12 T are well described at low T by the following model:

$$C = C_{el} + C_{KI} + \beta_D T^3 + DT^{-2}, \tag{1}$$

$$C_{el} = \gamma_0 T\left[(m^\star/m) + AT^2\ \ln\left(T/T^\star\right)\right], \tag{2}$$

here γ_0 in C_{el} is the 'bare' electronic coefficient of the specific heat expected from band structure, $m^*/m=\gamma(H)/\gamma_0$ is the many-body effective mass enhancement above the band mass m, A is a coupling constant dependent on the strength of the exchange interaction between Fermi-liquid quasiparticles and mass-enhancing excitations, D/T^2 is an empirically determined fitting term for the lowest temperature behavior, and T^* is the characteristic temperature for the excitations [22] We note that the $1/T^2$ form is a common high-temperature limiting behavior for a ground state multiplet, so its inclusion implies the existence of such a multiplet, possibly nuclear in origin, at temperatures much less than the lower limit of our data.

The three non-electronic terms in equation (2) include, first, a highly sample-dependent Schottky-like term $C_{\rm KI}$ arising from the temperature dependent screening of magnetic impurities in a Kondo insulator [5]. Numerically, the low and high temperature limits of this model closely match the standard Schottky expression for a two-level system with an energy gap Δ and ground state/excited state degeneracy ratio

$g_0/g_1 = 2$ [23]. We have therefore used the Schottky expression as a proxy for this model (which lacks a numerical prediction for intermediate temperatures). Second, we include a term $\beta_D T^3$ to represent the low temperature limit of the lattice specific heat in the Debye approximation (while at higher temperatures, the lattice contribution is fit to the full Debye model for the rigid hexaboride lattice plus a prominent Einstein-oscillator mode associated with Sm vibrations within a B_6 cage [24]). Third, we add an empirically fit DT^{-2} term to represent an anomalous upturn in C with decreasing T [25–27] analogous to but steeper than previously seen in heavy fermion systems [25–28]. Nuclear Schottky contributions observed at still lower temperatures in applied magnetic fields [27] have the same T^{-2} dependence but have been considered to be too small to be observed here in our data [7].

Turning now to the electronic contributions to the specific heat, we note the growing evidence for intrinsic low temperature magnetism in SmB_6 [29]. Thus, it is reasonable to expect an additional $T^3\ \ln(T/T^\star)$ contribution due to spin fluctuations, as previously observed in other Kondo systems [22], heavy fermions [30] and other electron mass-enhanced metals [31]. In SmB_6, the $T^3 \ln(T)$ term has previously been used to model the dependence of the low temperature specific heat of SmB_6 on carbon doping [32] and (La, Yb) rare earth substitution [33]. Specific heat measurements in a field can therefore provide a critical test: if spin fluctuations are the source of the zero field $T^3\ \ln(T/T^\star)$ contribution and mass enhancement $m^\star/m$, that enhancement should be significantly reduced for fields greater than or on the order of $H^* = \frac{k_B T^*}{\mu_B}$ where $k_B T^*$ is a characteristic energy for spin fluctuations. This reduction results in a decrease in the quasi-particle enhanced effective mass ratio $m^\star/m$ and thus $\gamma(H)$, which should be proportional to $(H/H^\star)^2$ at low fields [34, 35]. For $T^\star = 15$ K, $H^* = 23$ T.

Our observations at both low and high temperatures are consistent with the previously observed behavior discussed above. Consistent with this expectation, we find that C/T for all measured temperatures ($T \leqslant 1$ K) begins to significantly decrease above 18 T, leveling off above 22 T; the initial field dependence is proportional to $(H/H^*)^2$ (figure 1 inset). A low field Schottky peak around 1–2 T arises from the magnetic impurities present in the sample, as expected; we attribute a second peak seen in higher fields around 12–15 T to the experimentally observed suppression of the gap between the in-gap states and the conduction band [36] by a magnetic field on the order of 14 T.

Finally, we consider the oscillatory component of the specific heat. Normally such MQOs arise from the motion of charge carriers and here we are asking, irrespective of the nature of coupling to a gauge field, is there evidence for MQOs in the specific heat and thus the density of states? We show here that the answer is yes.

Magnetoquantum oscillations in thermodynamic quantities such as magnetization and specific heat that are periodic in inverse magnetic field arise from oscillations in the thermodynamic potential $\tilde{\Omega} = \tilde{\Omega}_0 f_T(z)$, where $\tilde{\Omega}_0$, is the zero temperature potential, $f_T(z) = z/\sinh z$ is a thermal smearing factor, and $z \equiv \pi^2 p\,(m^\star/m)\,(m/m_e)\,(k_B T/\mu_B H)$ is a dimensionless quantity proportional to effective mass, temperature, and inverse magnetic field. Here $m^\star$ denotes the quasi-particle interaction enhanced mass, m is the band mass, m_e is the bare electron mass, and p is an integer denoting the harmonic.

In the standard Lifshitz–Kosevich [L–K] model of MQO for a 3D Fermi surface [13] with extremal area A, the potential $\tilde{\Omega}_0$ and hence magnetization and specific heat are periodic in inverse field 1/H with a frequency of oscillation F in tesla given by $F = \left(\frac{\hbar}{2\ \pi e} A\right)$. The field and temperature dependent amplitude of the oscillatory specific heat corresponding to the pth harmonic of oscillation frequency F can be written as:

$$\tilde{C} = 2\ k_B \left(\frac{eH}{hc}\right)^{3/2} \frac{1}{|A''|^{1/2}} z f''(z) f_D p^{-3/2} \times \cos\left[2\pi p\left(\frac{F}{H} + \phi\right) \pm \frac{\pi}{4}\right], \tag{3}$$

where $A'' = |\partial^2 A(E_F)/\partial k^2|$ is a measure of the Fermi surface curvature, ϕ is a phase constant which may have any value between 0 and 1/2, and f_D is the Dingle factor $f_D = e^{-p\pi^2\ (k_B T_D^\star/\mu_B H)}$ [13, 14]. Here we have adopted the modern practice [13] of expressing f_D in terms of an effective mass $T_D^\star = (m^\star/m_e) T_D$ instead of the originally defined band mass temperature T_D [37, 38]. Importantly for the interpretation of the data presented here, $f_T''(z) = 0$ at $z \approx 1.61$, meaning there will be a node in the amplitude of the oscillatory specific heat as a function of magnetic field. Further, the field at which this node is observed is independent of oscillation frequency. As the value of z depends only on the temperature, magnetic field, and effective mass, the value of the effective mass can be directly determined from the node's location in field [16].

The size of the MQO in $C(T)$ predicted by this model for LaB_6 and SmB_6 are much smaller fraction of the total signal than the zero field electronic component of $C(T)$. In the small signal limit, a Fourier transform is needed to pull the signal out of the noise but to avoid introducing systematic errors in oscillation peak frequency identifications when performing the Fourier transform, it is necessary to use a more general non-uniform discrete Fourier transform technique known as the Lomb–Scargel (LS) method [39]. This method, widely used in astronomy, generates the uniform-in-$1/H$ data sets needed for accurate MQO frequency determination in a manner that avoids aliasing errors that would otherwise be introduced by more common interpolation techniques followed by a standard FFT. As with any Fourier transform method, it is also necessary to subtract off a smoothly varying uniform $C(H)$ background. To avoid the introduction of artificial low-frequency peaks, we fit the data to and then subtracted a non-oscillatory sigmoid function (rather than a simple polynomial expansion) before carrying out the frequency analysis.

As a test of our method, we first measured the oscillatory specific heat of a 0.085 μg sample of LaB_6. Applying the LS frequency analysis described above for a field sweep between 8 and 12 T at 0.358 K, we resolved sharp frequency peaks shown in figure 2: F = 847(±8), 1697(±18), 3228(±15), 7866(±16), and 15 732(±21) T, in excellent agreement with previously reported values of 845, 1690, 3220, 7800, and 15 600 T based on dHvA measurements [40, 41], plus a broad

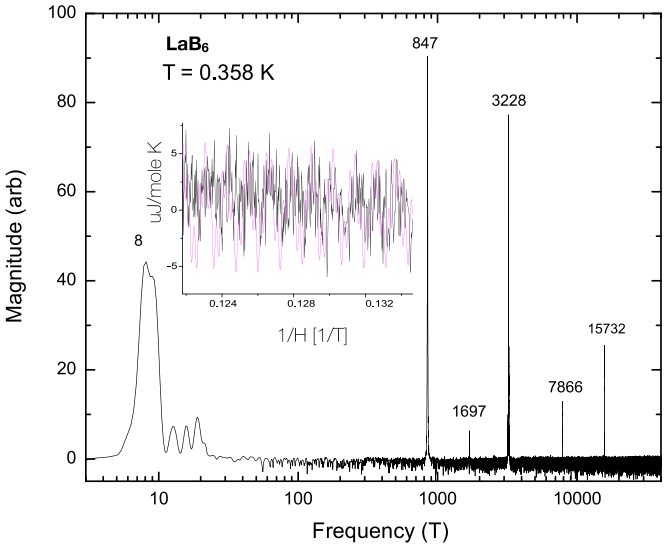

Figure 2. Fourier power spectrum indicating observed MQO oscillation frequencies for LaB6 in the [001] direction at 0.358 K between 8 and 12 T. Inset: inverse field dependence of oscillatory specific heat from which Fourier power spectrum was generated (in black), along with an L–K model fit to the data using the identified frequencies (in purple).

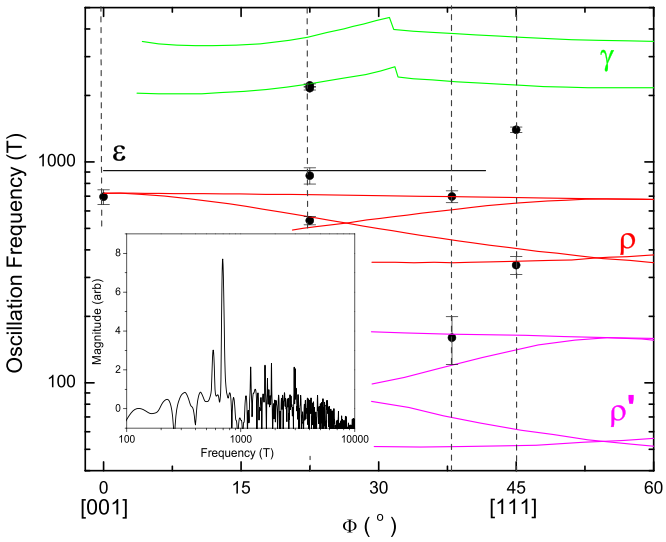

Figure 3. Angular dependence of the oscillation frequencies identified in the Fourier power spectrum for a 1.511 mg flux grown sample of SmB_6 (solid points) in fields up to 32 T. For clarity, we have included only the most prominent peak(s) observed in the Fourier power spectrum at each orientation. Solid lines correspond to predicted angle-dependent oscillation frequencies for SmB_6 [7]; the band labels ρ, ρ', ϵ, and γ are as presented there. Inset: a representative Fourier power spectrum for SmB_6 with a peak oscillation frequency of 695 T, in this case for a field oriented along [001]. Despite the inherently small size of the oscillatory specific heat for this material, the oscillation frequencies are readily identified, and are in good agreement with magnetic torque measurements and band structure predictions.

peak at approximately 8 T in fair agreement with oscillations reported at 4 T in magnetoresistance [40] and at 5 T in sound velocity [42, 43]. The small amplitude of the oscillations means the signal to noise ratio is low as a function of inverse magnetic field but the oscillation frequencies are readily and accurately identified using the LS frequency analysis method.

For SmB_6, we applied the same analysis method as used for LaB_6. The identified frequencies and their orientation dependence are in good agreement with previous results [7]. In figure 3 compare the predicted oscillation frequencies [2] (shown as green, black, red and pink lines) with frequencies determined from measurements of the oscillatory specific heat made between 18 and 31 T. For clarity, only the most prominent peaks in each Fourier power spectrum are shown. As can be seen by the Fourier power spectrum for a magnetic field oriented along [001] shown in the inset to figure 3, we are unable to clearly resolve the lowest expected oscillation frequencies in most cases but find an approximately 90% fidelity agreement at higher frequencies with the values reported for magnetic-torque measurements on float zone grown samples [7].

For confirmation of the observed MQOs in $C(H)$ of SmB_6, a second set of measurements were made on a 0.126 μg Al-flux grown sample using a high-resolution membrane nanocalorimeter [18], as shown in figure 4 for a field sweep at 0.52 K for $H \parallel [111]$ up to 12 T. In this field range, the data is best fit assuming $m^* = 6.6\ m_e$.

To determine the effective mass independent of fitting parameters, we can make use of our observation at higher magnetic field of a node in the magnetic-field-dependence of the MQOs [13, 16] at 0.58 K, for a field applied along [111]. At this orientation, we identify two prominent oscillation frequencies 341 T and 1399 T (as shown in figure 3). First, in figure 5(a),

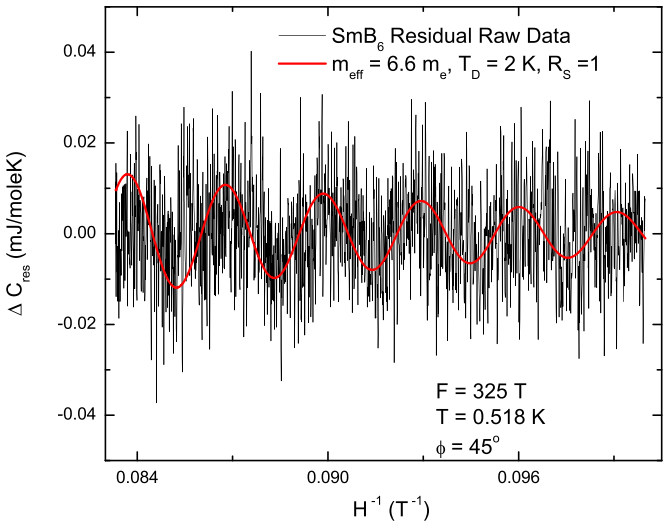

Figure 4. Oscillatory specific heat vs H^{-1} at T = 0.518 K for $\Phi = 45^\circ$ for a field sweep between 10 and 12 T. Data is shown in black. The red curve is the L–K prediction for the most prominent frequency of oscillation in the data (325 T) identified in the Fourier power spectrum at this orientation, with $m_{eff} = 6.6\ m_e$ and $T_D = 2$ K.

we illustrate the dependence of the location of the node in oscillatory specific heat on effective mass for a series of effective mass ratios. The location of the node is independent of oscillation frequency, so for clarity, these oscillations are

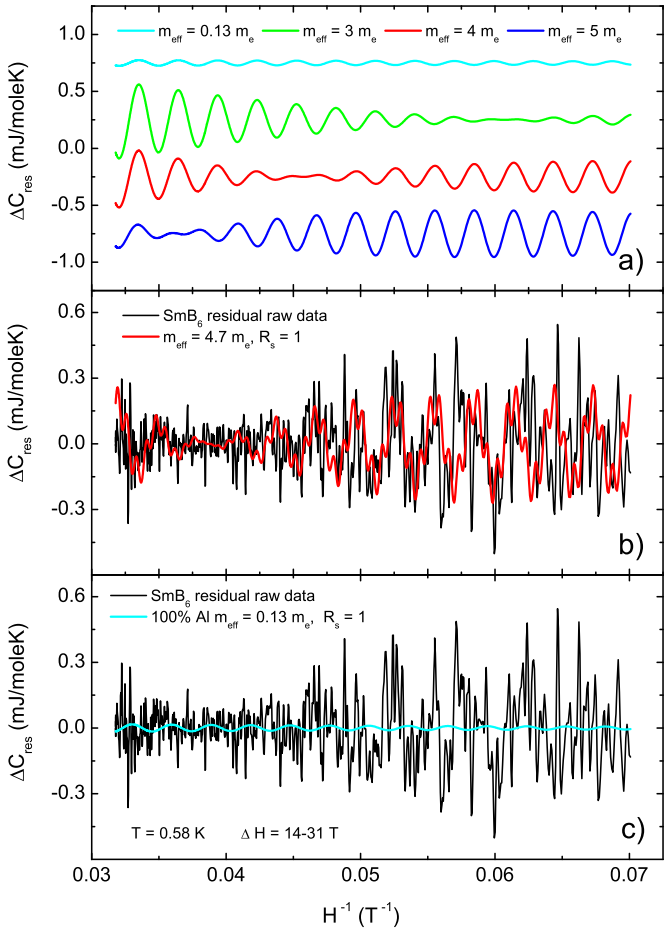

Figure 5. (a) Illustration of the dependence of the oscillatory specific heat on effective mass, for a sample temperature $T = 0.58$ K, a Dingle temperature $T_D = 1$K and an oscillation frequency $F = 341$ T, for effective mass enhancement ratios 0.13, 3, 4, and 5 respectively. Traces offset vertically for clarity. (b) Residual specific heat vs H^{-1} at $T = 0.58$ K and $\Phi = 45^\circ$. The red curve is a comparison of the data to a fit of the L–K model using an effective mass of 4.7 m_e determined from the node in the oscillatory specific heat and the two frequencies of oscillation (341 T and 1399 T) identified from the Fourier power spectrum at this orientation. (c) Comparison of the data with the L–K model prediction for a 100% Al sample with effective mass of $0.13m_e$ and $T_D = 1$ K. For all fits, we assume a spin splitting factor $R_S = 1$.

shown using a single oscillation frequency of 341 T. Second, in figure 5(b), we compare the original data (in black) with the prediction of the L–K model (in red) for an effective mass ratio of 4.7, this time including oscillations at both 341 T and 1399 T. The overall agreement is good but limited by the small size of the oscillations in the raw data. Nevertheless, inclusion of even just these two most prominent frequencies of oscillation captures much of the observed variation in amplitude with field, confirming our effective mass determination. The size of the decrease in the measured effective mass from 12 T to 24 T at this temperature parallels that seen for the field dependence of $\gamma(H)$.

One cause for caution when measuring flux grown samples is that they often possess Al inclusions, and torque measurements have shown such inclusions can produce MQOs at frequencies similar to those expected for SmB_6 [4]. For our flux grown samples, the absence of a discernible jump in the zero-field electronic specific heat of 1% or greater at the Al superconducting transition temperature of 1.163 K places an upper limit on the actual Al percentage of less than 5%. This is a critical test since, if Al inclusions are producing MQOs, then they must arise from high quality crystalline material. In figure 5(c) we therefore compare our measurements for the same trace as figure 5(b) with the corresponding oscillation amplitude and magnetic field dependence expected for an aluminum sample, using the known oscillation frequencies and effective masses of Al [44]. We see here that even at the 100% level (pure Al), we are unable to account for the amplitude of the MQOs we see in the specific heat. Further, the effective mass determined from location of the observed node in the amplitude of the oscillatory specific heat is incompatible with that which would be observed for aluminum, given an effective mass of 0.13 m_e. The MQO observed in our samples cannot arise from aluminum inclusions.

The large effective masses determined above are consistent with a recent first-principles, parameter-free all-electron electronic-structure model for SmB_6 ($\frac{m^*}{m} = 2.0$–22.0 depending on the band) [45], but are in contrast with values ranging from $\frac{m^*}{m} = 0.1$–1.0 found from torque magnetometry [1, 2, 7, 46]. One possible theoretical explanation for the discrepancy in effective mass values observed by specific heat and magnetic torque would be the simultaneous existence of light and heavy quasiparticle masses, as has been proposed for SmB_6 [47]. In this theoretical model, the MQOs arise when a highly asymmetric nodal semimetal forms at low temperature with carriers populated from disorder-induced in-gap states in small-gap Kondo insulators [48]. Whether this theory allows the formation of charge neutral excitations is not clear to us but in any case, it would be interesting if the theory were to be extended to include a calculation of the oscillatory specific heat, so as to enable a more direct comparison with our results. Additionally, recent experimental studies on the Kondo insulator YbB_{12} suggest a two-fluid picture for the origin of the observed MQO profile in which neutral quasiparticles coexist with charged fermions [49]. In future measurements, we hope to use still higher resolution calorimeters to measure $C(H,T)$ vs ϕ to probe for light and heavy effective masses in high quality flux and float-grown samples.

In conclusion we have resolved MQOs in the high field residual specific heat of SmB_6 that show good agreement with theoretical expectations for the dependence of oscillation frequency on crystallographic orientation for SmB_6, consistent with the existence of neutral quasiparticles at the Fermi surface. It has been shown in recent theoretical work that neutral quasiparticles arise naturally in mixed valence systems as Majorana excitations [12]. Such excitations would exhibit no charge transport in linear response, but would indeed show MQOs in magnetization, as well as specific heat, consistent with our observations. Further studies, in particular extending our measurements to lower temperatures, could allow accurate resolution of the peak attenuation factors expected to arise from spin splitting, which would in turn allow a confrontation with a Majorana interpretation of specific heat MQOs [12].

Data availability statement

The data that support the findings of this study are available upon reasonable request from the authors.

Acknowledgments

We would like to acknowledge the contributions of Dale Renfrow of the Smith College Center for Design and Fabrication and Ju-Hyun Park, William Coniglio, and Ali Bangura of NHMFL for technical support. The samples were grown at Los Alamos National Laboratory by P F Rosa.

This work was also supported in part by the U.S. Department of Energy Office of Basic Energy Science, Division of Condensed Matter Physics Grant DE-SC0017862 (P G L and A P R). A portion of this work was performed at the National High Magnetic Field Laboratory, which is supported by the National Science Foundation Cooperative Agreement No. DMR-1644779 and the State of Florida.

ORCID iDs

P G LaBarre https://orcid.org/0000-0001-9814-6486
N A Fortune https://orcid.org/0000-0002-2704-9969

References

[1] Li G *et al* 2014 *Science* **346** 1208
[2] Tan B S *et al* 2015 *Science* **349** 287
[3] Wolgast S, Eo Y S, Sun K, Kurdak I M C, Balakirev F F, Jaime M, Kim D J and Fisk Z 2017 *Phys. Rev.* B **95** 245112
[4] Thomas S, Ding X, Ronning F, Zapf V, Thompson J, Fisk Z, Xia J and Rosa P 2019 *Phys. Rev. Lett.* **122** 166401
[5] Fuhrman W T and Nikolić P 2020 *Phys. Rev.* B **101** 245118
[6] Li L, Sun K, Kurdak C and Allen J W 2020 *Nat. Rev. Phys.* **2** 463–79
[7] Hartstein M *et al* 2018 *Nat. Phys.* **14** 166–72
[8] Hartstein M, Liu H, Hsu Y T, Tan B S, Ciomaga Hatnean M, Balakrishnan G and Sebastian S E 2020 *iScience* **23** 101632
[9] Chowdhury D, Sodemann I and Senthil T 2018 *Nat. Commun.* **9** 1766
[10] Knolle J and Cooper N R 2015 *Phys. Rev. Lett.* **115** 146401
[11] Knolle J and Cooper N R 2017 *Phys. Rev. Lett.* **118** 096604
[12] Varma C M 2020 *Phys. Rev.* B **102** 155145
[13] Shoenberg D 1984 *Magnetic Oscillations in Metals* (Cambridge: Cambridge University Press)
[14] Sullivan P F and Seidel G 1968 *Phys. Rev.* **173** 679–85
[15] Fortune N A, Brooks J S, Graf M J, Montambaux G, Chiang L Y, Perenboom J A A J and Althof D 1990 *Phys. Rev. Lett.* **64** 2054–7
[16] Bondarenko V A, Uji S, Terashima T, Terakura C, Tanaka S, Maki S, Yamada J and Nakatsuji S 2001 *Synth. Met.* **120** 1039–40
[17] Stankiewicz J, Evangelisti M, Rosa P F S, Schlottmann P and Fisk Z 2019 *Phys. Rev.* B **99** 045138
[18] Tagliati S, Krasnov V M and Rydh A 2012 *Rev. Sci. Instrum.* **83** 055107
[19] Fortune N A and Hannahs S T 2014 *J. Phys.: Conf. Ser.* **568** 032008
[20] Fortune N, Gossett G, Peabody L, Lehe K, Uji S and Aoki H 2000 *Rev. Sci. Instrum.* **71** 3825–30
[21] Rosa P F S and Fisk Z 2021 Bulk and surface properties of SmB_6 *Rare-Earth Borides* ed D S Inosov (New York: Jenny Stanford Publishing) ch 11
[22] Ikeda K, Dhar S, Yoshizawa M and Gschneidner K 1991 *J. Magn. Magn. Mater.* **100** 292–321
[23] Gopal E 1966 *Specific Heats at Low Temperatures* (Berlin: Springer)
[24] Mandrus D, Sales B C and Jin R 2001 *Phys. Rev.* B **64** 012302
[25] Flachbart K, Gabáni S, Gloos K, Konovalova E, Orendac M, Paderno Y, Pavlik V, Reiffers M and Samuely P 2002 *Physica* B **312–313** 379–80
[26] Gabáni S, Flachbart K, Konovalova E S, Orendác M, Paderno Y B, Pavlík V and Sebek J 2001 *Solid State Commun.* **117** 641–4
[27] Flachbart K, Gabáni S, Neumaier K, Paderno Y, Pavlík V, Schuberth E and Shitsevalova N 2006 *Physica* B **378–380** 610–1
[28] Stewart G R 2001 *Rev. Mod. Phys.* **73** 797–855
[29] Gheidi S, Akintola K, Akella K, Côté A, Dunsiger S, Broholm C, Fuhrman W, Saha S, Paglione J and Sonier J 2019 *Phys. Rev. Lett.* **123** 197203
[30] Stewart G R, Fisk Z, Willis J O and Smith J L 1984 *Phys. Rev. Lett.* **52** 679–82
[31] Brinkman W and Engelsberg S 1968 *Phys. Rev.* **169** 417–31
[32] Phelan W, Koohpayeh S, Cottingham P, Freeland J, Leiner J, Broholm C and McQueen T 2014 *Phys. Rev.* X **4** 031012
[33] Orendáč M, Gabáni S, Pristáš G, Gažo E, Diko P, Farkašovský P, Levchenko A, Shitsevalova N and Flachbart K 2017 *Phys. Rev.* B **96** 115101
[34] Hertel P, Appel J and Fay D 1980 *Phys. Rev.* B **22** 534–41
[35] Béal-Monod M T and Daniel E 1983 *Phys. Rev.* B **27** 4467–70
[36] Caldwell T, Reyes A P, Moulton W G, Kuhns P L, Hoch M J R, Schlottmann P and Fisk Z 2007 *Phys. Rev.* B **75** 075106
[37] Dingle R B 1952 *Proc. R. Soc.* A **211** 500–16
[38] Dingle R 1952 *Proc. R. Soc.* A **211** 517–25
[39] VanderPlas J T 2018 *Astrophys. J. Suppl. Ser.* **236** 16
[40] Arko A J, Crabtree G, Karim D, Mueller F M, Windmiller L R, Ketterson J B and Fisk Z 1976 *Phys. Rev.* B **13** 5240–7
[41] Ishizawa Y, Tanaka T, Bannai E and Kawai S 1977 *J. Phys. Soc. Japan* **42** 112–8
[42] Suzuki T, Goto T, Fujimura T, Kunii S, Suzuki T and Kasuya T 1985 *J. Magn. Magn. Mater.* **52** 261–3
[43] Thalmeier P, Lemmens P, Ewert S, Lenz D and Winzer K 1987 *Europhys. Lett.* **4** 1177–81
[44] Larson C O and Gordon W L 1967 *Phys. Rev.* **156** 703–15
[45] Zhang R, Singh B, Lane C, Kidd J, Zhang Y, Barbiellini B, Markiewicz R S, Bansil A and Sun J 2020 arXiv:2003.11052 [cond-mat]
[46] Xiang Z, Lawson B, Asaba T, Tinsman C, Chen L, Shang C, Chen X and Li L 2017 *Phys. Rev.* X **7** 031054
[47] Harrison N 2018 *Phys. Rev. Lett.* **121** 026602
[48] Shen H and Fu L 2018 *Phys. Rev. Lett.* **121** 026403
[49] Xiang Z *et al* 2021 *Nat. Phys.* **17** 788–93